Generation of Simplified Protein Raman Spectra Using Three-Color Picosecond Coherent Anti-Stokes Raman Spectroscopy

Paul M. Donaldson,[†,§] Keith R. Willison,[‡] and David R. Klug*[,†]

The Single Cell Proteomics Group, Chemical Biology Centre, Department of Chemistry, Imperial College London, Exhibition Road, London, SW7 2AZ, United Kingdom, and Institute of Cancer Research, Chester Beatty Laboratories, Section of Cell and Molecular Biology, London SW3 6JB, United Kingdom

Received: July 3, 2010

The well-known and prominent marker bands of aromatic amino acids in Raman spectra of protein and peptide films are revisited in the frequency and time domains using three-color picosecond coherent anti-Stokes Raman spectroscopy (CARS). We show here that control of the probe delay allows the narrow width/long lifetime states to be observed free not only from nonresonant background and fluorescence contamination but also free from the spectral congestion that arises from the complex background of spectrally broader (shorter lifetime) vibrational modes. The reasonable limits of detection obtained indicate that such CARS methods may be useful for quantitative analysis of protein composition.

Introduction

The relative and absolute quantification of proteins and their amino acid composition from separated cell extracts is of central importance in the field of proteomics. The possibility of performing such analyses by optical means, on proteins separated, for example, by capillary electrophoresis (CZE) or high-performance liquid chromatography (HPLC) and deposited on a suitable substrate is of great practical interest. It is well established that vibrational spectroscopy can isolate spectral features from proteins which report on secondary structure, amino acid composition and chemical state.[1−5] Spectroscopic signals usually have a simple relationship to the quantity of material present in the sample meaning that in principle additional labeling/tagging is not necessary for quantification of protein levels. It is also possible in principle to identify proteins from their amino acid composition. It therefore follows that key requirements for a vibrational spectroscopic method to become useful as a protein identification method are high sensitivity, sufficient information content, and elimination of spectral congestion/backgrounds.

An optical method for direct protein differentiation/identification and absolute copy number quantification was recently outlined based on determining the amino acid composition of a set of proteins by measuring the amino acid vibrational band strengths relative to the CH_2/CH_3 stretch bands.[6,7] To circumvent the usual problems of spectral congestion and contaminating backgrounds a type of picosecond two-dimensional infrared spectroscopy known as EVV-2DIR, based on infrared-infrared-visible four wave mixing,[8−12] was employed to completely isolate background/congestion free signals from a CH_3 band, phenylalanine (F), tyrosine (Y), and tryptophan (W). In this way it was possible to determine the relative quantities of three amino acids in a protein and the method also allowed the absolute quantification of protein levels. A defining feature of 2D-IR spectroscopy that helped to reduce spectral congestion of the protein spectra was the ability to select only coupled vibrational states (the fundamental feature of multidimensional vibrational spectroscopy). The method also employed picosecond delays between the excitation pulses to reduce the levels of nonresonant background relative to the desired signals.[9]

In this paper we show that even in one-dimensional spectroscopies the pulse delays themselves can filter out broad (short-lived) vibrational states and so reduce spectral congestion. We explore how this factor alone contributes to the simplification of peptide and protein spectra through 3-color picosecond coherent anti-Stokes Raman spectroscopy (CARS). The use of probe delays for the simplification of CARS spectra is demonstrated for dried peptide and protein films. For the systems examined, we show that probe delays greater than 1.4 ps for 1 ps Gaussian half-width pulses generate excellent quality CARS spectra of protein aromatic amino acids, with the narrow bands of W, F, and Y clearly isolated from the numerous broader protein vibrational modes. Probe delay scans are used to recover the line-widths of the bands, and we also explore experimental detection limits, measuring F signals from the protein bovine serum albumin (BSA) at levels in the tens of femtomoles range ($\sim 10^{10}$ BSA molecules in the laser focus).

Protein films are studied here for several important reasons. When a protein or peptide solution is deposited on a nonwetting substrate, it dries in a nonuniform manner resulting in a thin ring of solid material with an annular width as low as a hundred micrometers. This concentrating effect has been used in ordinary Raman spectroscopy to allow small volumes of low concentration protein solution to be analyzed.[13] An additional advantage of dried protein films is that they can be made in the form of continuous "tracks" from separation methods such as CZE and HPLC[13−15] allowing laser spectroscopic methods to conveniently and efficiently probe the resulting protein fractions. For coherent nonlinear optical applications such as EVV 2D-IR spectroscopy and CARS, such sampling methods remove the requirement for a sample cell with a front window and containing solvent, significantly reducing the nonresonant background contribution to the signal.

* To whom correspondence should be addressed. Phone: +0044 (0)20 7594 5806. E-mail: d.klug@imperial.ac.uk.
† Imperial College London.
‡ Institute of Cancer Research.
§ Present address: Physikalisch-Chemisches Institut, Universität Zürich, Winterthurerstrasse 190, CH-8057 Zürich, Switzerland.

10.1021/jp1061607
Published on Web 08/30/2010

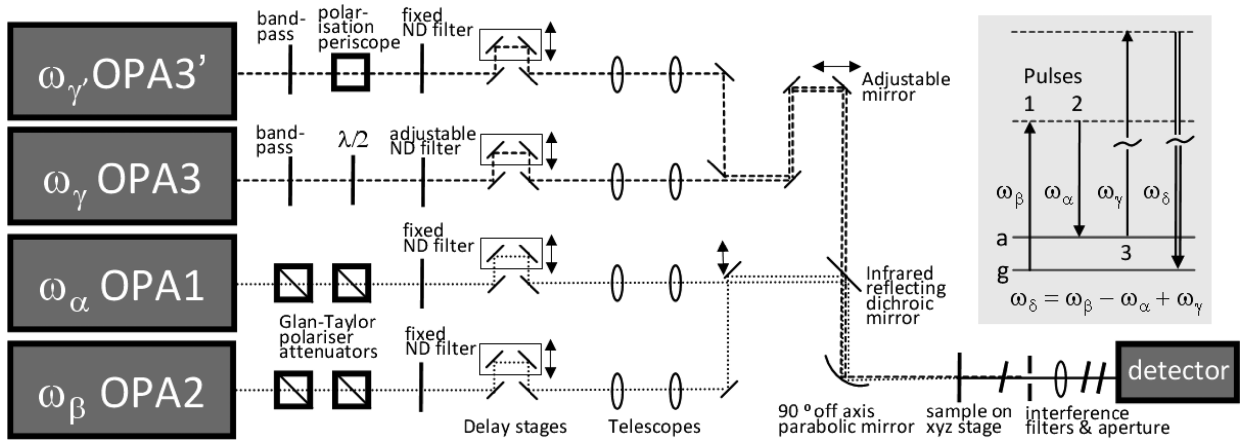

Figure 1. Experimental layout and wave mixing diagram (shaded box) describing the three-color picosecond CARS experiments reported in this paper.

The important parameter that many ultrafast CARS techniques allow control of is the delay between the Stokes pump pulses and the anti-Stokes probe pulse. Such delays are used to reduce the nonresonant background contribution to the CARS signal,[16] accurately measure vibrational linewidths in the time domain,[17] achieve additional levels of contrast in CARS microscopy,[18,19] and as a means of performing Fourier transform CARS spectroscopy.[20] Many interesting methods of performing delayed probe CARS spectroscopy exist.[21−24] Our investigations focus on the picosecond three-color method.[25] The wave-mixing diagram depicting three-color CARS is shown in Figure 1. For the experiments reported in this paper, three independently tunable picosecond laser pulses are used for the Stokes pump pulses 1 and 2 (frequencies ω_β, ω_α) and the anti-Stokes probe pulse 3 (ω_γ).The separation in wavelength of the output signal $\omega_\delta = \omega_\beta - \omega_\alpha + \omega_\gamma$ from the input laser pulses removes the problem of scatter from the input pulses. By use of standard perturbative methods,[26,27] we write the CARS signal for a vibrational transition **g** to **a** as a third order polarization generated by the three pulses

$$P(t) = N\alpha_{ga}C_\gamma(t)e^{i\omega_\delta t}\frac{i}{\hbar}\int_0^\infty dt_1\alpha_{ag}e^{i(\omega_{ga}-\omega_\beta+\omega_\alpha)t_1-\Gamma_{ag}t_1}\times C_\alpha(t-t_1+T_{23})C_\beta(t-t_1+T_{13}) \quad (1)$$

Each field $E(t)$ is expressed as the product of an envelope and a carrier: $C(t)e^{i\omega t}$. The pulse 1−3 delay is T_{13} and pulse 2−3 delay T_{23}. We note that a recent paper by Mukamel[28] offers a more efficient way to calculate the CARS polarization for arbitrary pulse shapes.

The interpretation of eq 1 is as follows. Pulsed fields 1 (ω_β) and 2 (ω_α) generate a vibrational polarization of size dictated by the Raman polarizability α_{ag}. For the case of a purely homogeneously broadened line the polarization generated at any point in time decays exponentially with a rate Γ_{ag} or lifetime $\tau_{ag} = \Gamma_{ag}^{-1}$ The total vibrational polarization is calculated by summing over the decaying polarizations generated at all times t_1 earlier than t. Pulsed field 3 (ω_γ) acts at time t on the vibrational polarization and generates the radiating third-order CARS polarization $P(t)$, the size of which is determined by the amount of vibrational polarization at time t, the polarizability α_{ga}, and N, the number density of chromophores probed. For this paper, pulse 2 is fixed, and pulses 1 and 3 scanned in time. The relationship between the probe delay T and T_{12} and T_{23} is shown in Figure 2. For the measurements in this paper we use

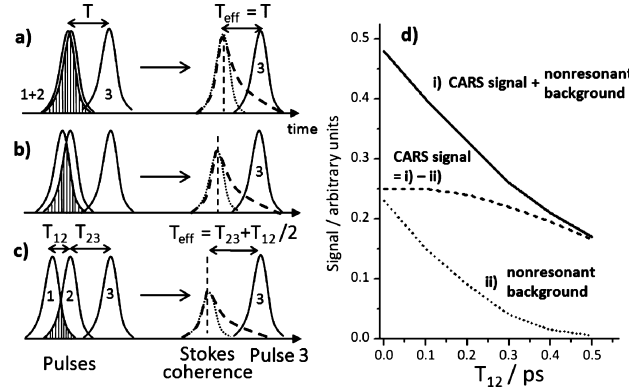

Figure 2. Three-color CARS pulse delays. (a) Conventional pulse arrangement for three-color CARS. Also depicted is the Stokes coherence generated by pulses 1 and 2, relative in time to pulse 3. (b) and (c) Effect of a slight delay between the Stokes pulses, with pulse 2 fixed in time. (d) CARS signal from BSA deposited on a glass coverslip. (i) Resonant (F, 1005 cm^{-1}) and (ii) nonresonant signals are plotted as a function of T_{12} delay along with their difference as a function of T_{12} delay ($T_{23} = 1$ ps).

relatively narrow-band picosecond pulses to record spectra in the frequency domain and linewidths in the time domain. We detect the total signal intensity:

$$I(\omega_\alpha, \omega_\beta, \omega_\gamma, T_{12}, T_{23}) \propto \int_{\text{pulse3}} |P(t)|^2 dt \quad (2)$$

Our application of the three-color CARS method to protein spectra simplification is straightforward. The signals from the pure electronic polarization (nonresonant background) and Raman features of line width greater than the laser pulse bandwidth all decay with the envelope of the pulses and therefore make no contribution to the CARS signal when Stokes pulses 1 and 2 are not overlapped with probe pulse 3. Thus, for 20 cm^{-1} laser pulse bandwidths, Raman features with homogeneous or inhomogeneous linewidths greater than this amount will not appear in probe delayed spectra. For the Raman bands with linewidths less than 20 cm^{-1} (i.e., a lifetime τ_{ag} longer than the pulse duration), increasing the probe delay selectively filters out the signals from shorter lived modes that appear in the frequency domain spectrum. The effectiveness of the filter, of course, depends on the total and relative strengths of the Raman bands of interest. For complicated Raman spectra such as those of the proteins presented in this paper, we show that

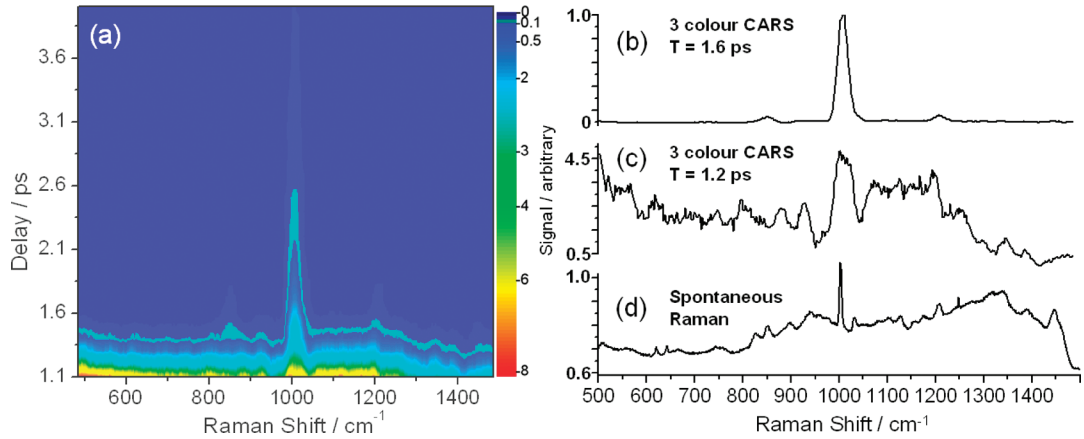

Figure 3. (a) Color plot showing three-color picosecond CARS spectra of a BSA film as a function of probe beam delay *T*. (b) A probe delay of $T = 1.6$ ps provides almost complete rejection of the complex background of short-lived protein modes in the CARS spectrum leaving only Y and F spectral features. The complexity of the protein spectrum without such a "filter" can be seen in the $T = 1.2$ ps CARS spectrum of (c). The spontaneous Raman spectrum of the BSA sample is shown in (d). The CARS spectra were recorded with 2.5 cm^{-1} step sizes and 500 samples per point. Graph (a) was recorded with a 0.1 ps step size.

the use of a probe delay as a "line width filter" offers different "views" of a Raman spectrum and allows us to reveal spectra of the strong and narrow aromatic bands not only fluorescence free but with greatly reduced spectral congestion inherent to ordinary Raman spectroscopy.

Experimental Section

The three-color CARS spectra presented in this paper were recorded using a general purpose picosecond/femtosecond nonlinear spectroscopy platform comprising 4 computer-controlled white light seeded optical parametric amplifiers (OPA, Spectra Physics OPA800C) pumped by a 3 Watt 1-kHz regenerative amplifier (Spectra Physics Spitfire Pro XP) producing pulses of ~1 ps fwhm duration and ~20 cm^{-1} bandwidth. Computer automated wavelength calibration and scanning was added to each OPA, with calibration carried out using an Oriel MS257 Monochromator. Each OPA was equipped with an optical delivery line containing a telescope, polarisers, filters, and a computer-controlled delay stage. The overall experimental layout is shown in Figure 1. CARS spectra were recorded with OPA3 or 3′ fixed as a probe and OPAs 1 and/or 2 scanned in frequency across the Raman shift range of interest.

Selection of the operating wavelengths for generating three-color CARS signal involved consideration of factors such as sample damage thresholds, nonlinear backgrounds, the requirement of pulses 1 and 2 to generate Raman shifts from 500−3300 cm^{-1}, available bandpass filtering for laser pulse rejection and also the peak quantum efficiency of the detector. A Hamamatsu H7422−40 photomultiplier (quantum efficiency 25% at 600 nm) was used to detect the CARS signals through a gated integrator in analogue and photon counting modes. Stokes pulses 1 and 2 were typically the signal from one OPA (6200−8400 cm^{-1}) and the idler from another OPA (5300−6150 cm^{-1}). Pulse 3 was sourced from one of two OPAs and varied between 633 and 790 nm (second harmonic of the signal or the 790 nm pump light). Detection of CARS signals in the 3000-cm^{-1} range was carried out using a 790-nm probe beam, allowing the signal to remain in the same 600−650-nm detection bandwidth as the ~1000 cm^{-1} up-shifted signals generated from the 650 nm probe beam. The Stokes pulses were polarized vertically with respect to plane of propagation. The anti-Stokes pulse polarization was horizontal, reducing the nonresonant background by around 70%. The phase matching angles for each beam were fully adjustable; however, a near-collinear geometry was used in the experiments reported here, making easier the attainment of beam spatial overlaps and tight focusing at the sample position. All excitation beams were focused using a single 15 cm focal length 90 degree off axis parabolic mirror and the focal spot sizes at the sample matched by control of input beam diameters, giving focused spot sizes of 40−50 μm in diameter (fwhm).

Careful attenuation of the input beam energies using neutral density filters and adjustable polarizer cubes was necessary in order to avoid sample damage. Typically, 100−200 nJ of 633 nm and 500−750 nJ of near-IR light was used per pulse at the beam focus. After setting attenuation levels, if sample damage was still observed during a measurement, a convenient and unobtrusive means of reducing the peak intensity of Stokes pulses 1 and 2 was to introduce a delay between the two pulses. Figure 2 demonstrates that such a T_{12} delay also increases the signal to nonresonant background ratio in exactly the same manner as that of a probe beam T delay (Figure 2a). As the vibrational polarization is maximum at times exactly halfway between pulses 1 and 2, T_{12} delays also modify the probe delay. For all data in this paper we quote an effective probe delay $T = T_{\text{eff}} = T_{23} + T_{12}/2$. Due to the > 5mm thickness of the BBO crystals used, scanning the OPA output frequencies caused changes in the pulse delays and also the beam displacements/divergence. The delay shifts were corrected during spectral acquisitions by automatically adjusting the timing of each pulse using a pre-measured calibration curve.

The proteins and peptides examined in this paper were typically prepared in pure water at concentrations in the micro- to millimolar range and deposited in volumes of between 0.3 and 1 μL onto 100 μm thick glass coverslips. Experiments for determining detection limits were performed using a 4 μm thick PTFE film (Goodfellow) as the substrate. The peptides were obtained from synthesis procedures described previously[29] and the proteins were obtained from Sigma-Aldrich. Raman spectra were recorded using a Horiba Jobin Yvon LabRam Infinity Raman microscope with 633 nm excitation.

Results and Discussion

The use of three-color picosecond CARS spectroscopy in decongesting protein spectra is well illustrated by taking the example of BSA, shown in Figure 3. When the delay between the Stokes pump pulses and the anti-Stokes probe pulse is close

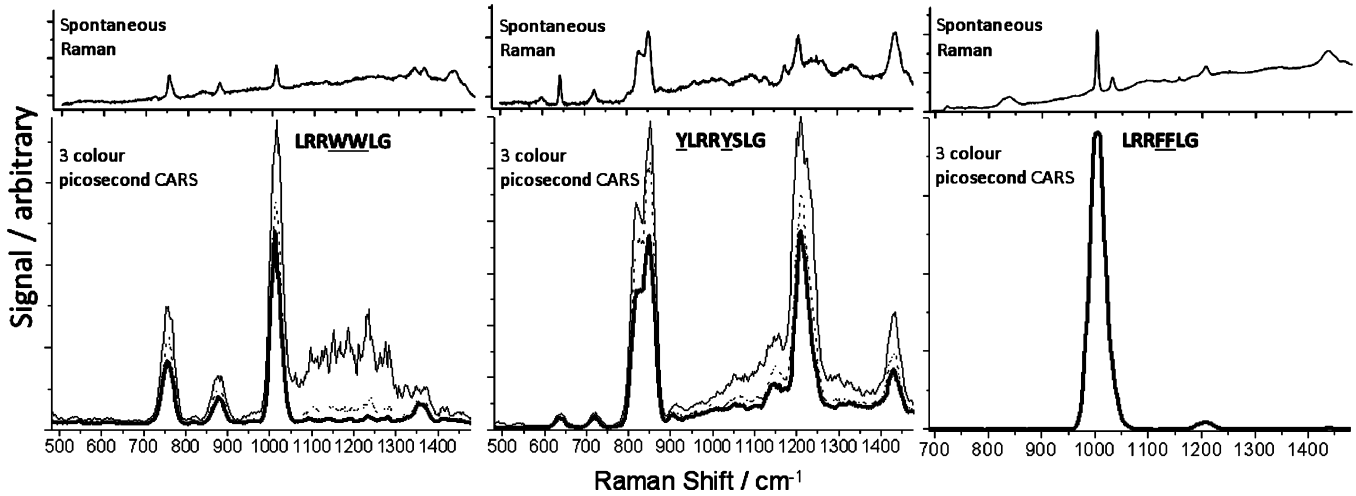

Figure 4. Spontaneous Raman (upper plots) and three-color CARS spectra (lower plots) of peptides containing W, Y, and F. The solid-line CARS spectra of these peptides were collected with probe delays of 1.9, 1.7, and 1.7 ps, respectively. The LRRWWLG and YLRRYSLG graphs also show two delays 0.1 and 0.2 ps earlier. Whereas the CARS spectra are all background free, the spontaneous Raman spectra have background levels of roughly 50−60% of the signal maxima.

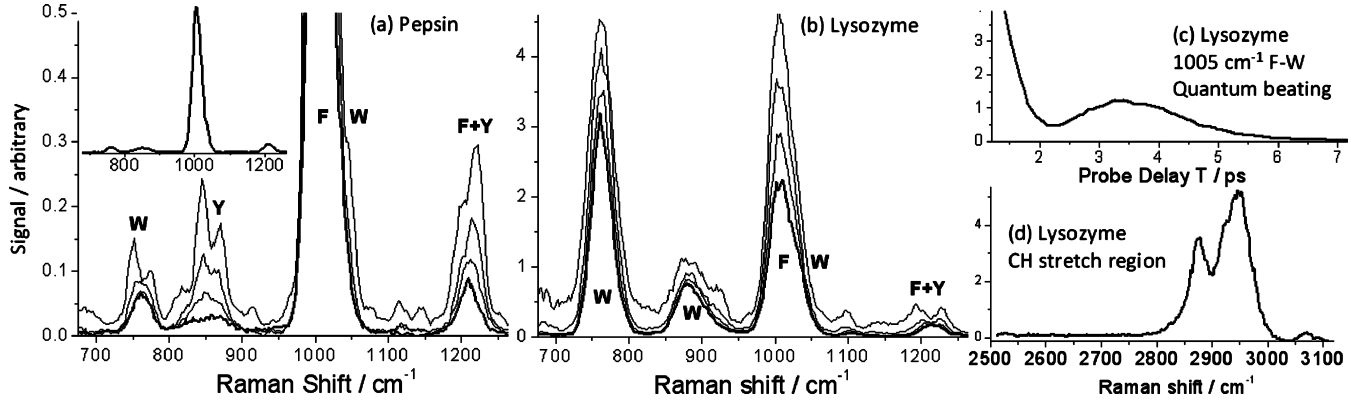

Figure 5. Three color picosecond CARS spectra of films of (a) pepsin and (b) lysozyme. Four different probe delays (a) 1.6, 1.8, 2.0, 2.2 ps and (b) 1.4, 1.5, 1.6, 1.7 ps are shown. (c) Beating between F and W signals in a 1005-cm^{-1} Stokes shift probe delay scan. (d) Lysozyme CARS signal in the CH stretch region recorded with a 1.6-ps probe delay.

to zero, the CARS signal is dominated by the nonresonant background. With probe delays greater than 1.2 ps (slightly larger than the laser pulse-widths), the signal is mostly CARS. Figure 3a depicts a series of spectra taken with increasing probe delay. Only three bands at 850, 1005, and 1210 cm^{-1} contribute to the spectrum for delays greater than 1.5 ps and are attributable to Y, F, and F + Y, respectively. Each peak is, in the frequency domain, broadened by the ∼20 cm^{-1} bandwidth 1-ps pulses. The $T = 1.6$ ps spectrum of Figure 3b shows that three-color CARS can generate a spectrum of the Y and F modes in BSA completely free of the complicated background of shorter lived vibrational modes present in the $T = 1.2$ ps spectrum of Figure 3c. The 400 fs additional delay required to remove the complicated bandshapes corresponds to a 4x reduction of 1005 cm^{-1} F signal. The spontaneous Raman spectrum of the same BSA sample in Figure 3d shows that the F peak is sitting on a broad, complex signal, where the apparent baseline comprises a background that is 50% of the peak signal.

To confirm the BSA spectrum assignments and address the issue of what kind of spectral content might be accessible with probe-delayed three-color CARS protein spectra, Y-, F-, and W-substituted peptides (LRRWWLG, YLRRYSLG, LRRFFLG, and YGFF) were examined. The Raman modes of Y, F, and W are discussed extensively in the literature.[1−3,30,31] Our investigations mainly examined the spectral regions of 500−1400 and 2700−3100 cm^{-1}. Figure 4 shows representative CARS data compared with spontaneous Raman spectra of the same peptide samples. The spectra clearly show which Y, F, and W Raman bands can be spectrally isolated with picosecond pump delays. The most prominent features of the LRRWWLG spectrum are the 760, 880, 1015, and 1360 cm^{-1} W bands. The LRRYYLG data shows Y peaks at 645 (weak), 830/850 cm^{-1} (the so-called Fermi doublet), and 1210 cm^{-1}. The LRRFFLG spectrum shows F features at 1005 and 1210 cm^{-1}.

In addition to the BSA data of Figure 3, measurements on lysozyme (chicken egg white) and pepsin (porcine gastric mucosa) were made, with relevant data shown in Figure 5. In a similar manner to the decongestion of the BSA spectrum, probe delays greater than ∼1.4 ps gave CARS signals mainly due to the aromatic amino acids, with the complicated background of other protein modes suppressed. The aromatic amino acid compositions of BSA, lysozyme, and pepsin are shown in Table 1. BSA contains very little W; hence only features due to F and Y are obvious in the CARS spectrum. Lysozyme and pepsin on the other hand contain larger amounts of W, and its contributions are clearly observable in their CARS spectra. It is clear that the 760 cm^{-1} W band is well isolated with respect to the other bands. On the other hand, for the 20 cm^{-1} bandwidth picosecond laser pulse experiments reported here, the F and W bands at 1006 and 1015 cm^{-1} are not well resolved. The lysozyme spectral data around 1000 cm^{-1} clearly shows the 1015 cm^{-1} W band as a shoulder on the F band. Both bands are

TABLE 1: Number of Aromatic Amino Acid Residues per Protein and Percent Compositions for BSA, Lysozyme (Chicken Egg White), and Pepsin (Porcine Gastric Mucosa)

	Phe (F)	Tryp (W)	Tyr (Y)
BSA	27 (4.6%)	2 (0.3%)	20 (3.4%)
lysozyme	3 (2.3%)	6 (4.7%)	3 (2.3%)
pepsin	14 (4.3%)	5 (1.5%)	16 (4.9%)

excited by the Stokes pulse on resonance, giving rise to a beating of the CARS signal in probe delay scans, as shown in Figure 5c. The contribution of W to the 1005 cm^{-1} F band can be removed, albeit with a loss of signal by exciting the F band on the red side. Another way of achieving the separation would be to use narrower bandwidth Stokes pulses (possibly shaped for a fast falling edge) or use a broadband pump, narrow band probe, and spectrally dispersed signal. The lysozyme spectrum of Figure 5 (b) shows that the strong 880 cm^{-1} W signal can easily overwhelm the Y Fermi doublet signal. The only other observable Y band is at 1210 cm^{-1}, which also overlaps with an F band.

Figure 5d shows a spectrum of the lysozyme CH stretch region around 3000 cm^{-1}. Alongside the strong aliphatic band, a peak thought to be due to aromatic CH stretch is clearly observable at ~3160 cm^{-1}. Although small compared with the aliphatic peak, it is comparable in size to the 1005 cm^{-1} F band and could therefore be useful as a piece of information in amino acid composition analysis. On the basis of photomultiplier signal levels, the aliphatic CH stretch peaks were at least one hundred times as strong as the aromatic bands in the 1000-cm^{-1} region. It was of great interest to use these strong aliphatic CH and aromatic CH stretch signals as internal standards to check whether the aromatic signals in the 700−1200 cm^{-1} range were reliable indicators of protein composition as was previously demonstrated using 2D IR spectroscopy.[6] For the experiments reported here however, a reliable measurement of W or F and CH-stretch signal ratios was not possible because the 2000-cm^{-1} jump in OPA2 output between the two spectral regions caused beam displacements and changes in beam divergence. This resulted in the two differently focused sets of laser pulses sampling slightly different areas of the protein rings, giving strongly position dependent signal ratios.

Although the three-color picosecond CARS method used here was limited in spectral resolution by the 20-cm^{-1} bandwidth excitation pulses, probe delay scans could be used to make accurate measurements of vibrational linewidths. For aromatic amino acids it is not known how widely the linewidths vary from protein to protein. As we are proposing that the use of a probe delay can render certain bands background free to report quantitatively on information such as amino acid composition, it is important that for the bands of interest the variation is not significant. Figure 6 shows logarithmic probe delay scans of the peak CARS intensities from some of the bands studied, along with lifetimes τ extracted from the linear fits. The strong linearity in the data shows that these bands, as expected, are homogeneously broadened. The data set shows decay times τ ranging from 1.2 to 3.4 ps corresponding to Raman linewidths between 3 and 11 cm^{-1}. One can see that the 760 cm^{-1} W band from an LRRWWLG peptide has a similar lifetime to the W bands from lysozyme and pepsin. There is a difference of a few hundred femtoseconds between the lifetime of the 1005-cm^{-1} F band observed from BSA and from the peptide YGFF. BSA and pepsin F lifetimes are similar, but beatings from weak W contributions are present in the pepsin 1005-cm^{-1} F band plot. The lifetime of the 1015 cm^{-1} W band is more than half that of

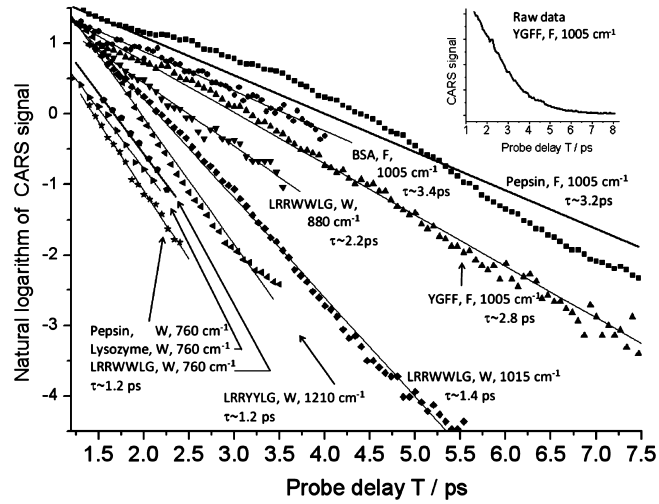

Figure 6. Logarithmic protein and peptide three-color CARS signal vs probe delay. The driven part of the CARS response ($<T = 1.1$ ps) are not included in the plots. The intensity decay time τ for each plot is indicated. Each signal decays as $e^{-2\Gamma t}$ (see top-right inset graph for YGFF). Here, $\tau = 1/\Gamma$, where Γ is the slope of the linearized signal decay. To separate the plots, each line has been shifted along the *y*-axis, so the relative intensities of each plot are arbitrary and should be ignored.

the nearby 1005 cm^{-1} F bands, potentially useful in removing W signal from the 1005 cm^{-1} F band measurement.

Figures 3− 5 clearly demonstrate background free measurements of W, Y, and F bands from dried protein and peptide films with the three-color CARS method. Whether or not this is might be useful in an analytical context ultimately depends on what kind of limit of detection is attainable for these bands. Our method of estimating a limit of detection was as follows. Protein samples of known concentration were deposited as droplets of known volume onto 4 μm thick PTFE film stretched over a lens mount and dried into rings <1 mm in diameter. The 4 μm PTFE substrate was used as it had a nonresonant background 1000 times smaller than 100 μm thick glass. The wavelengths of the Stokes pump pulses 1 and 2 were set to drive the 1005-cm^{-1} F transition, and the samples were then moved in the laser focus on an *xy* stage to record three-color CARS signal "images" of the droplets, as shown in Figure 7.

The 1005-cm^{-1} F band CARS signals of Figure 7a were generated from BSA solution droplets dried from 0.3 μL volumes at concentrations of 30 μM (top row) and 10 μM (bottom row). The signal size depends on the protein number density squared (eqs 1 and 2), so the square root of the signal from each pixel is shown in Figure 7. The total signal from each ring was determined by summing the pixels in an area containing one ring and subtracting the background, giving total signal levels ~3 times higher for the 30 μM droplets compared with the 10 μM droplets, as expected. The signal-to-noise ratio for a pixel on the 30 μM droplets was between 7 and 14. An example CARS spectrum of the F peak with signal-to-noise ratio of 7 is shown in Figure 7c. The CARS signal is clearly sitting on a background of ~50 photons s^{-1}, which derives mainly from the probe pulse being inadequately rejected at the detector. Against this background, the 10-μM droplets of Figure 7a show a per pixel signal-to-noise of ~1−1.5. If this background were removed in future experiments with more effective filtering, the 10 μM droplets would show a signal-to-noise of 3−4. We can estimate the sensitivity of the CARS experiment for F in terms of protein numbers as follows. Figure 7b shows three 10-μM droplets, still with the 50 s^{-1} background but collected with a

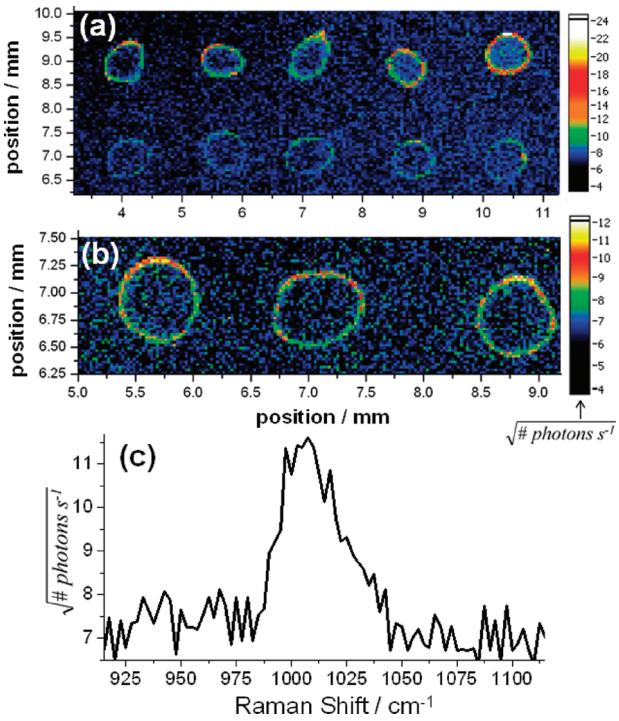

Figure 7. Three-color picosecond CARS image of 1005 cm^{-1} phenylalanine signal from BSA protein droplets dried into rings from 0.3 μL of solution on a 4 μm thick PTFE film. All signal sizes are shown on the same scale (square root of the number (#) of photons s^{-1}). The probe delay was $T = 1.25$ ps. The incident pulse frequencies were $\omega_\beta = 5105$ cm^{-1}, $\omega_\alpha = 4100$ cm^{-1}, and $\omega_\gamma = 15722$ cm^{-1} (636 nm). Each pixel is an average of 1000 laser pulse samples. (a) Image of five 30-μM drops (top row) and five 10-μM drops (bottom row) recorded with a 50-μm step size. (b) Image of three 10-μM drops recorded with 25-μm step-size. Shown in (c) is a CARS spectrum recorded from a pixel of a 30 μM droplet showing a peak signal of 11 (photons $s^{-1})^{1/2}$ and signal-to-noise ratio of 7.

step size of 25 μm, roughly equal to the area from which the CARS signal is generated (estimated from the individual laser spot sizes). Assuming that most of the dried protein from the 0.3 μL drops is drawn into the rings upon drying, each ring corresponds to a total of $\sim 2 \times 10^{12}$ BSA molecules. Each ring has $\sim 125 \pm 25$ pixels with clear CARS signal. This means that the signal from each pixel on average derives from $\sim 2 \times 10^{12} \div 125 = \sim 1.5 \times 10^{10}$ molecules.

In addition to the 50 photons s^{-1} of unrejected probe light, the design and performance of our CARS experiment was far from optimized. The sub-micro-Joule excitation pulses required for these CARS experiments could easily be generated from higher repetition rate amplifiers. Use of a higher efficiency (gated) charge-coupled device camera would increase the signal size by 2−3 times, and experimentation with pulse durations, focusing, wavelength, bandwidth, and pulse-shape might also yield further improvements in detection limits, spectral isolation and resolution. The limit of detection measured here for F in 10 μM BSA from 0.3 μL solution is approaching that achieved by Ben-Amotz and co-workers for 15 μm inkjet microprinted drops of lysozyme using ordinary Raman spectroscopy, albeit with two differences.[13] Each BSA molecule has 27 F residues, compared with 3 for lysozyme. The F signal in the study of Ben-Amotz was measured recording an entire spectrum with 100-s signal averaging, as opposed to the 1-s signal averaging used in this work to measure the single peak intensity of the 1005 cm^{-1} F band. Such single frequency (single-point) intensity measurements are an efficient means of performing protein composition analysis using a few vibrational bands.[6]

Conclusions

In this paper we have demonstrated a new application of picosecond three-color CARS spectroscopy for generating simplified protein Raman spectra. The data in this paper illustrates the basic point that broad vibrational bands can be selectively removed from a spectrum by adjusting the probe delay. A protein CARS spectrum recorded with a probe delay of 1.2 ps, although containing a favorable balance of signal to nonresonant background, was found to be significantly congested; however an additional delay of 400 fs could remove the complicated band shapes. For the proteins BSA, pepsin, and lysozyme, simplified, high-quality CARS spectra of the aromatic amino acid bands were observed. By use of concentrated dried protein rings on thin substrates, significant reductions in nonresonant background signals were made, yielding sensitivities approaching the femtomole range for phenylalanine residues in BSA.

The ability to isolate the 760 cm^{-1} W mode is clearly of potential use in quantitative amino acid analysis. Although the 1005 cm^{-1} F and 1015 cm^{-1} W modes overlapped in our data, these two bands could in principle still be distinguished in future CARS experiments. The ability to observe the Y 830/850 cm^{-1} Fermi resonance band could be useful in structure/environment studies; however, quantitative determination of Y for protein identification may be less straightforward. Not only is the 830/850-cm^{-1} Fermi resonance band environmentally sensitive it appears to be easily dominated by the 880-cm^{-1} W band. The 1210-cm^{-1} Y band has an equivalent overlapping F band at exactly the same strength and frequency. That the three-color CARS experiment does not appear to be able to clearly isolate Y over a spectral range of 600 cm^{-1} demonstrates the remarkable achievement of earlier 2D-IR measurements, which clearly isolated narrow W, F, and Y cross peaks deriving from IR bands in the 1475−1550 cm^{-1} region over a 2D spectral range of just 150 by 150 cm^{-1}.[6,7] However, the quality of the three-color CARS data and the reasonable (and improvable) signal-to-noise levels demonstrated in this paper indicate that probe-delayed three-color CARS could form a useful component in the kind of optical platform for protein differentiation/identification envisaged in our earlier 2D-IR studies.

Acknowledgment. This research was supported by the EPSRC and BBSRC (EP/C54269X/1) through the Single Cell Analysis Project of Imperial College London.

References and Notes

(1) Kitigawa, T.; Hirota, S. *Handbook of Vibrational Spectroscopy*; Wiley: New York, 2003; Vol. 5.
(2) Tu, A. T. Peptide backbone conformation and microenvironment of protein side chains. In *Spectroscopy of Biological Systems*; Clark, R. J. H., Hester, R. E., Eds.; John Wiley and Sons Ltd: New York, 1986.
(3) Fabian, H.; Anzenbacher, P. *Vib. Spec.* **1993**, *4*, 125.
(4) Barth, A. *Prog. Biophys. Mol. Biol.* **2000**, *74*, 141.
(5) Barth, A.; Zscherp, C. *Q. Rev. Biophys.* **2002**, *35*, 369.
(6) Fournier, F.; Gardner, E. M.; Kedra, D. A.; Donaldson, P. M.; Guo, R.; Butcher, S. A.; Gould, I. R.; Willison, K. R.; Klug, D. R. *Proc. Natl. Acad. Sci. U. S. A.* **2008**, *105*, 15352.
(7) Fournier, F.; Guo, R.; Gardner, E. M.; Donaldson, P. M.; Loeffeld, C.; Gould, I. R.; Willison, K. R.; Klug, D. R. *Acc. Chem. Res.* **2009**, *42*, 1322.
(8) Zhao, W.; Wright, J. C. *Phys. Rev. Lett.* **2000**, *84*, 1411.
(9) Meyer, K. A.; Wright, J. C. *Anal. Chem.* **2001**, *73*, 5020.
(10) Donaldson, P. M.; Guo, R.; Fournier, F.; Gardner, E. M.; Barter, L. M. C.; Barnett, C. J.; Palmer, D. J.; Gould, I. R.; Willison, K. R.; Klug, D. R. *J. Chem. Phys.* **2007**, *127*, 114513.
(11) Donaldson, P. M.; Guo, R.; Fournier, F.; Gardner, E. M.; Gould, I. R.; Klug, D. R. *Chem. Phys.* **2008**, *350*, 201.
(12) Guo, R.; Fournier, F.; Donaldson, P. M.; Gardner, E. M.; Gould, I. R.; Klug, D. R. *Phys. Chem. Chem. Phys.* **2009**, *11*, 8417.

(13) Zhang, D. M.; Xie, Y.; Mrozek, M. F.; Ortiz, C.; Davisson, V. J.; Ben-Amotz, D. *Anal. Chem.* **2003**, *75*, 5703.
(14) He, L.; Natan, M. J.; Keating, C. D. *Anal. Chem.* **2000**, *72*, 5348.
(15) Amantonico, A.; Urban, P. L.; Oh, J. Y.; Zenobi, R. *Chimia* **2009**, *63*, 185.
(16) Kamga, F. M.; Sceats, M. G. *Opt. Lett.* **1980**, *5*, 126.
(17) Laubereau, A.; Kaiser, W. *Rev. Mod. Phys.* **1978**, *50*, 607.
(18) Volkmer, A.; Book, L. D.; Xie, X. S. *Appl. Phys. Lett.* **2002**, *80*, 1505.
(19) Lee, Y. J.; Cicerone, M. T. *Appl. Phys. Lett.* **2008**, *92*.
(20) Ogilvie, J. P.; Beaurepaire, E.; Alexandrou, A.; Joffre, M. *Opt. Lett.* **2006**, *31*, 480.
(21) Cheng, J. X.; Xie, X. S. *J. Phys. Chem. B* **2004**, *108*, 827.
(22) Rinia, H. A.; Bonn, M.; Muller, M. *J. Phys. Chem. B* **2006**, *110*, 4472.
(23) Pestov, D.; Murawski, R. K.; Ariunbold, G. O.; Wang, X.; Zhi, M. C.; Sokolov, A. V.; Sautenkov, V. A.; Rostovtsev, Y. V.; Dogariu, A.; Huang, Y.; Scully, M. O. *Science* **2007**, *316*, 265.
(24) Katz, O.; Natan, A.; Silberberg, Y.; Rosenwaks, S. *Appl. Phys. Lett.* **2008**, *92*, 171116.
(25) Laubereau, A.; Laenen, R. Ultrafast Coherent Raman and Infrared Spectroscopy of Liquid Systems. In *Ultrafast Infrared and Raman Spectroscopy*; Fayer, M. D., Ed.; Marcel Dekker: New York, 2001.
(26) Mukamel, S. *Principles of Nonlinear Spectroscopy*, 1st ed.; Oxford University Press: Oxford, 1995.
(27) Mukamel, S. *Annu. Rev. Phys. Chem.* **2000**, *51*, 691.
(28) Mukamel, S. *J. Chem. Phys.* **2009**, *130*, 054110.
(29) Fournier, F.; Gardner, E. M.; Guo, R.; Donaldson, P. M.; Barter, L. M. C.; Palmer, D. J.; Barnett, C. J.; Willison, K. R.; Gould, I. R.; Klug, D. R. *Anal. Biochem.* **2008**, *374*, 358.
(30) Jenkins, A. L.; Larsen, R. A.; Williams, T. B. *Spectrosc. Acta A* **2005**, *61*, 1585.
(31) Fischer, W. B.; Eysel, H. H. *Spectrosc. Acta* **1992**, *48A*, 725.

JP1061607